ELSEVIER

Fuel Processing Technology 87 (2006) 935 – 942

FUEL PROCESSING TECHNOLOGY

www.elsevier.com/locate/fuproc

Pyrolysis of palm oil wastes for enhanced production of hydrogen rich gases

Haiping Yang [a,*], Rong Yan [b], Hanping Chen [a], Dong Ho Lee [b],
David Tee Liang [b], Chuguang Zheng [a]

[a] State Key Laboratory of Coal Combustion, Huazhong University of Science and Technology, Wuhan, 430074, P. R. China
[b] Institute of Environmental Science and Engineering, Nanyang Technological University, Innovation Center,
Block 2, Unit 237, 18 Nanyang Drive, Singapore 637723, Singapore

Received 18 December 2005; received in revised form 18 May 2006; accepted 10 July 2006

Abstract

A study on pyrolysis of palm oil wastes in a countercurrent fixed bed was carried out, aiming to characterize the hydrogen rich gas products in view of enhanced energy recycling. The effects of temperature, residence time and catalyst adding on the yields and distribution of hydrogen rich gas products were investigated. The main gas species generated, as identified by Micro-GC, were H_2, CO, CO_2, CH_4 and trace amounts of C_2H_4 and C_2H_6. With temperature increasing from 500 °C to 900 °C, the total gas yield was enhanced greatly and reached the maximum value (~70 wt.%, on the raw biomass sample basis) at 900 °C with big portions of H_2 (33.49 vol.%) and CO (41.33 vol.%). Residence time showed a significant influence on the upgrading of H_2 and CO_2 yields. The optimum residence time (9 s) was found to get a higher H_2 yield (10.40 g/kg (daf)). The effect of adding chemicals (Ni, γ-Al_2O_3, Fe_2O_3 and La/Al_2O_3, etc.) on gas product yield was investigated and adding Ni showed the greatest catalytic effect with the maximum H_2 yield achieved at 29.78 g/kg (daf).

Keywords: Palm oil wastes; Temperature; Pyrolysis; Hydrogen; Catalyst adding

1. Introduction

Pyrolysis is one of the most promising thermo-chemical conversion routes to recover energy from biomass. During pyrolysis, biomass is thermally decomposed to solid charcoal, liquid oil and H_2-rich gases under an oxygen absence condition. The yields of end products of pyrolysis and the composition of gases are dependent on several parameters including temperature, biomass species, particle size, heating rate, operating pressure and reactor configuration, as well as the extraneous addition of catalysts [1,2]. Temperature and residence time, as the two most important parameters [3,4], have been investigated widely in bench scale reactors including fixed beds [5], fluidized beds [6], and others [7]. Generally, H_2-rich gas products are favored at a high temperature and long residence time. The highest yield of H_2 (12.65 wt.%) and 91% energy conversion efficiency were obtained from biomass pyrolysis with adding of catalyst [8]. Although the H_2 yield from the direct pyrolysis of biomass is quite low, it was known that the gas yield, especially H_2 yield, could be highly improved by catalyst adding [2,9]. So far, various types of chemicals, such as dolomite ($CaCO_3 \cdot MgCO_3$), K_2CO_3, Na_2CO_3, Ni/Al_2O_3, Fe_2O_3, Rh/CeO_2/M (M = SiO_2, Al_2O_3, and ZrO_2), etc. were selected as catalysts to improve the overall efficiency of the system in producing high quality fuel gases, so as to increase the economic feasibility of the biomass pyrolysis/gasification process [10–13]. Furthermore, the inorganic mineral matters presenting in biomass, as they contain a large amount of alkali metals or alkaline-earth metals (like Ca, K, Na, Mg, etc.), could also show a great catalytic effect on gaseous products from biomass pyrolysis/gasification [11,14].

Palm oil wastes are the main biomass resources in ASEAN countries. In Malaysia and Indonesia, the two largest palm oil producing countries in the world, there were 30 M ton and 8.2 M ton of palm oil wastes (empty fruit bunch, fiber, palm oil shell) generated respectively in year 2000, and they are increasing at spectacular pace with the rapidly expanding of food and manufacturing industries. To treat this tremendous amount

---

[*] Corresponding author. Tel.: +86 27 87542417; fax: +86 27 87545526.
E-mail address: yhping2002@163.com (H. Yang).

0378-3820/$ - see front matter © 2006 Elsevier B.V. All rights reserved.
doi:10.1016/j.fuproc.2006.07.001

Table 1
Proximate and ultimate analyses of palm oil shell

	Proximate analysis (wt.%)				Ultimate analysis (wt.%, dry basis)					LHV (MJ/kg)	Molecular formula
	M_{ad}	V_{ad}	A_d	FC_{ad}	C	H	N	S	O [a]		
Shell	5.73	73.74	2.21	18.37	53.78	7.20	0.00	0.51	36.30	22.14	$CH_{1.61}O_{0.51}$
Fiber	6.56	75.99	5.33	12.39	50.27	7.07	0.42	0.63	36.28	20.64	$CH_{1.69}O_{0.54}$
EFB	8.75	79.67	3.02	8.65	48.79	7.33	0.00	0.68	40.18	18.96	$CH_{1.80}O_{0.62}$

M: moisture content; *V*: volatile matters; *A*: ash; FC: fixed carbon; ad: on air dried basis; d: on dry basis.

[a] The oxygen (O) content was determined by difference.

of wastes, novel technologies with improved efficiencies and reduced environmental impacts need to be established timely.

It was found in our previous study using TGA–FTIR that palm oil wastes could be ideal biomass sources for biofuel production [15]. In this study, the pyrolysis of palm oil wastes was investigated using a countercurrent fixed bed reactor under different operating conditions (temperature, residence time, catalyst adding), in order to achieve an improved performance of palm oil wastes conversion to energy with a higher yield of H_2-rich gases.

2. Materials and methods

2.1. Samples

The three palm oil wastes (shell, fiber and empty fruit bunches — EFB) were obtained from Malaysia. They were ground in a laboratory-scale centrifugal mill (Rocklabs, New Zealand) and sieved in a Retsch test sieve with a 1-mm screen (Retsch, Fisher Scientific Company, USA), i.e. the particle size of the sample analyzed is less than 1 mm. The results of proximate and ultimate analysis of palm oil wastes are listed in Table 1, showing that palm oil wastes are environment friendly energy sources containing trace amount of N, S and mineral matters. If considering only the main elements (C, H, O), the molecular formula of the studied samples based on one C atom can be written as CH_xO_y, as listed in Table 1.

Seven types of pure chemicals (purity ~99.99%), including K_2CO_3, $CaMg(CO_3)_2$, Na_2CO_3, Ni, γ-Al_2O_3, Fe_2O_3 and La/Al_2O_3, were introduced in the thermal system as catalyst to improve the yields of gas product from biomass pyrolysis. These chemicals had an average diameter of 0.1 mm or less. Their BET surface areas were measured using ASAP2010 with liquid N_2 at 77 K. It was found that K_2CO_3 and Na_2CO_3 contain very low surface areas (<1 m^2/g) while those of Ni, $CaMg(CO_3)_2$, La/Al_2O_3 and Fe_2O_3 are higher (2–9 m^2/g), γ-Al_2O_3 shows the highest surface area (151.7 m^2/g). The catalysts were directly dry-mixed with biomass samples [11] and the weight ratio of catalyst to biomass (*C*/*W*) is kept at 0.05.

2.2. Experimental set-up and methods

Pyrolysis of biomass materials was conducted in a bench scale countercurrent fixed bed shown in Fig. 1. The system consists essentially of a quartz tube (ID 50 mm, OD 55 mm, bed height 41 cm, and air freeboard 21 cm) with a continuous feeding system, a gas cleaning section containing a cyclone solid collector and a quartz wool filter, and a cooling system for the separation of water and condensable organic vapors (tar), as well as various gas measurement

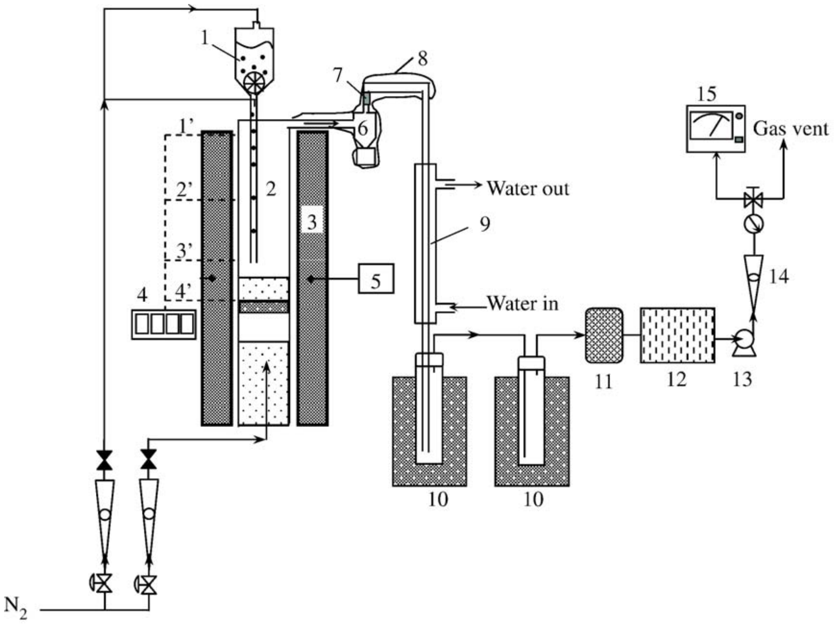

Fig. 1. The flow scheme of bench scale reactor. 1. Screw feeder, 2. fixed bed, 3. furnace, 4. thermocouples (1′, 2′, 3′, 4′), 5. temperature controller, 6. cyclone particle collector, 7. fiber filter, 8. heating tapes, 9. water cooler, 10. ice-water condenser I, II, 11. particle filter (glass wool), 12. gas dryer (silica gel), 13. pump, 14. flow meter, and 15. gas analyzer (Micro-GC, FTIR).

devices. Purge gas (N_2) was supplied from the bottom of the reactor at a flow rate of 5 l/min.

The ground palm oil wastes were held in a hopper with a motor feeder. A small flow of N_2 was used to blow the biomass powder in the entrainment tube into the reactor. To prevent biomass from degradation, the feeding tube is cooled by means of an air-cooled jacket. The feedstock (biomass) entering into the reactor is heated up, dried, devolatilized, and finally decomposed following Eq. (1) to generate solid charcoal, liquid tar, water vapor and H_2-rich gas products (H_2, CO, CO_2, CH_4, etc.). The operating pressure in the reactor was atmospherically controlled by a vacuum pump. To mitigate the influence of sample feeding on the temperature profile in the reactor, the feeding rate was kept at ~1 g/min, the experiment lasted for 30 min.

$$\text{Biomass}\rightarrow\text{Gas}(H_2, CO, CO_2, C_mH_n) + H_2O + \text{tar} + \text{char} \quad (1)$$

The solid charcoal residue was mostly collected on the screen sieve (air distributor). The volatiles and fine particles, carried by purging gas, passed through the cyclone and quartz wool filter and as such the fine particles were removed. The condensable was quenched when gas passed through a water-cooling tube and two ice-water condensers in series. After every experiment, the residues collected inside the tube and the cyclone were combined and recorded as solid charcoal. The cooling tube and condensers were weighed and the weight difference before and after the experiment was recorded as the liquid yield. The total gas yield (wt.%) could thus be calculated by the difference based on the mass balance of the fed biomass in a specific time period at a constant feeding rate. The condenser and all connection tubes were then washed using acetone and the liquid was also collected for further analysis. Those incondensable gases were pre-cleaned through a glass wool filter and dried by silica gels prior to analysis.

In this study, the total gas yield (wt.%) was experimentally determined by measuring the total gas volume and the gas density. The gas volume was checked by the gas flow meter. The volume mean density of gas products was determined based on the gas components at stable experimental conditions (generally 5–10 min after the sample feeding). According to this method, the sum of solid charcoal, liquid oil and gas product in our experiments is in the range of 88.2–95.2%; the rest of the parts (11.8–4.8%) could be some incondensable liquid oil, moisture and fine particles (adsorbed by silica gel gas dryer or glass wool particle filter). As the difference is only 11.8–4.8% (<12%), the method of determining pyrolysis gas product yield is reasonable. In most cases, only the gas yields were determined to reflect the effects of different parameters, as the focus of this study is to upgrade the quality and enhance the yield of gas products.

The gas products were analyzed using a dual Channels Micro-Gas Chromatograph (Micro-GC, Varian, CP-4900) with a thermal conductive detector (TCD). The two columns used are: (1) column A: Molecular sieve 5A (MS-5A), Ar carrier gas for analysis of H_2, CH_4, and CO at 95 °C; (2) column B (Porapak Q — PPQ, He carrier gas) for the analysis of CO_2 and some hydrocarbons (C_2H_4 and C_2H_6) at 60 °C. The yield of individual gas species (in volume, at 1 atm and 25 °C) was calculated for most runs based on the feeding rate, gas volume generated and gas components analyzed by Micro-GC. The H_2 yield (in weight) is then obtained from the molar volume (24.45 l per molar at 1 atm and 25 °C); in the following texts the yield of H_2 in unit of g/kg of biomass is used mostly for an easy comparison.

The liquid oil was further investigated using FTIR (BioRad Excalibur Series, model FTS 3000) equipped with a deuterated triglycine sulfate (DTGS) detector. The collected liquid oil was dissolved with 100 ml acetone solution, and 2 ml of the solution was put evenly on a KBr pellet. After vaporizing acetone, a thin film of liquid oil on the KBr plate was formed, and it was used for scanning. Before each measurement, the FTIR was run to establish a background with KBr while adding 2 ml of pure acetone was taken as reference. In this study, IR spectra were recorded between 4000 and 500 cm^{-1} with a resolution of 4 cm^{-1} and sensitivity of 1.

2.3. Thermodynamic calculation

The thermodynamic equilibrium calculation is independent of reactor to predict the possible maximum yield of final products, based on the minimization of the Gibbs free energy of the system [16]. The calculations of palm oil wastes pyrolysis were performed using HSC-Chemistry 4.0 software [17]. The final products involved are H_2, CO_2, CO, CH_4, H_2O and C. Referring to Table 1, the inputs of shell are: C — 1 mol, H — 1.61 mol, O — 0.51 mol; of EFB are: C — 1 mol, H — 1.8 mol, O — 0.62 mol; and of fiber are: C — 1 mol, H — 1.69 mol, O — 0.54 mol. Operating temperature is 900 °C, pressure is 1 atm. As the space is limited, the software was not introduced in detail here. Details of the thermodynamic calculation including equations and system design for computation could be found in our previous report [18].

3. Results and discussions

3.1. Influence of temperature on shell pyrolysis

The yields of final products from shell pyrolysis under different temperatures are listed in Table 2. With temperature increasing from 500 to 900 °C, the total gas yield increased sharply from 36.59 to 64.47 wt.% while both liquid and char yields reduced straightly. Meanwhile, varying temperature shows a great influence on gas product components. The main gas products are H_2, CO and CO_2, CH_4 and some C_2 hydrocarbons (C_2H_4 and C_2H_6). Among them, the H_2 content increased steadily from 3.56 to 15.04 vol.% as temperature increased from 500 to 800 °C, and with a further increase of temperature to 900 °C, the H_2 content increased significantly to 33.49 vol.% (i.e., 10.40 g/kg, daf). Yields of CH_4 also increased from 2.84 to 11.92 vol.% whilst that of CO_2 decreased in general with temperature increasing, particularly at 900 °C. The yield of CO decreased first from 36.77 to 22.12 vol.% as temperature increased to 700 °C, however it increased again to 41.33 vol.% as temperature continuously increased to 900 °C. The yields of C_2H_4 and C_2H_6 are relatively small and the influence of temperature is insignificant. At low temperature (500 °C), CO_2 (54.01 vol.%) and CO (36.77 vol.%) have the highest yields whilst CO (41.33 vol.%) and H_2 (33.49 vol.%) have the highest yields at high temperature (900 °C).

The thermal cracking of gas-phase hydrocarbons at high temperature might explain the variation of gas product distribution observed [3]. At high furnace temperature, prior to being quenched in the condenser, the gas species generated from biomass pyrolysis could undergo further reactions (secondary reactions) such as tar cracking and shifting reaction, leading to much more incondensable gases (including H_2) generated. Therefore, the total yield of gas products increased significantly as temperature increased from 500 °C to 900 °C. The main reactions involved could be expressed using the following Eqs. (2)–(10) [3,19]. Among them, Eqs. (3) and (8) are favored at lower pressure whilst Eq. (7) is favored at higher pressure, and Eq. (6) is favored at higher temperature (>1000 °C). The gas-phase steam reforming of methane (3) cannot proceed at 900 °C, but with the presence of catalyst the reaction (3) might possibly proceed on catalytic surface. In terms of increasing H_2 production, Eqs. (4), (5), (9) and (10 are the main reactions of interest for biomass pyrolysis at atmospheric pressure and temperatures between 600 °C and 900 °C. In contrast to H_2, other gas components might increase or decrease with the occurring of secondary reactions. As a result, Dai et al. [3] pointed out that the changing trend of H_2 concentrations can reflect the extent of secondary reactions; more H_2 generation suggests that

Table 2
Product yields and distribution from shell pyrolysis at different temperatures

Temp (°C)	Pyrolysis products (wt.%)			Components of the gas product (vol.%, N_2- and H_2O-free)						LHV of gas product (MJ/m^3)
	Char	Liquid	Gas	H_2	CO	CH_4	CO_2	C_2H_4	C_2H_6	
900	10.18	20.09	64.47	33.49	41.33	11.92	10.78	2.46	0.02	14.67
800	13.00	25.68	51.61	15.04	30.09	7.91	44.41	2.22	0.33	9.87
700	17.73	26.80	48.94	12.58	22.12	7.76	54.06	2.79	0.69	9.14
600	19.61	27.01	41.55	7.03	36.22	5.51	48.95	1.80	0.49	8.75
500	29.04	29.99	36.59	3.56	36.77	2.84	54.01	2.25	0.56	7.82

the secondary reactions occur significantly. From the above analysis, it can be concluded that higher temperature (900 °C) is favorable for thermal cracking of tar and shift reaction.

$$\mathrm{Tar} \rightarrow CH_4 + H_2O + C_mH_n + H_2 \tag{2}$$
$$CH_4 + H_2O \rightarrow CO + 3H_2 \tag{3}$$
$$C + H_2O \rightarrow CO + H_2 \tag{4}$$
$$CO + H_2O \rightarrow CO_2 + H_2 \tag{5}$$
$$C + CO_2 \rightarrow 2CO \tag{6}$$
$$C + 2H_2 \rightarrow CH_4 \tag{7}$$
$$CH_4 + CO_2 \rightarrow 2CO + 2H_2 \tag{8}$$
$$C_mH_n + 2nH_2O \rightarrow nCO_2 + [2n + (m/2)]H_2 \tag{9}$$
$$C_mH_n + nH_2O \rightarrow nCO + [n + (m/2)]H_2 \tag{10}$$

The lower heating value (LHV, KJ/m^3) of the gas products can be calculated using the following equation [3].

$$\begin{aligned} \mathrm{LHV} = {} & (30.0 \times CO + 25.7 \times H_2 + 85.4 \times CH_4 \\ & + 151.3 \times C_nH_m) \times 4.2 \end{aligned} \tag{11}$$

where CO, H_2, CH_4 and C_mH_n are the molar ratio of the CO, H_2, CH_4 and hydrocarbon (C_2H_4 and C_2H_6) in the gas product. The calculated results are also shown in Table 2. The heating value of total gas products increased straightly as the temperature increases. At 900 °C, LHV of gas products reached 14.67 MJ/m^3, which belongs to the medium level of heat values for gas fuels that can be directly used for gas engine, gas turbine or boiler for power generation. Also, it can be used for the chemical formation of methanol and methane, etc. [20].

The FTIR spectra of liquid oil from shell pyrolysis at different temperatures are illuminated in Fig. 2 shown in transmittance ratio. The O–H stretching vibration between 3300–3600 cm^{-1} (500 °C) and ~1300 cm^{-1} of liquid oils indicated the presence of alcohols and phenols. The presence of C=O stretching vibration between 1680 and 1718 cm^{-1} is compatible with the presence of ketone, quinine, aldehyde groups, etc. Symmetrical and asymmetrical C–H stretching vibration of aliphatic CH_3 and CH_2 groups (2870–2960 cm^{-1}), C–H bending vibrations between 1380 and 1465 cm^{-1} indicated the presence of alkane groups in pyrolysis oil derived from biomass. CH_3 group located at 1390 cm^{-1} is extremely valuable for the detection of methyl group. The small transmittance peak observed at 1645 cm^{-1} implied the existence of C=C (alkenes). Furthermore, mono and polycyclic aromatic groups are

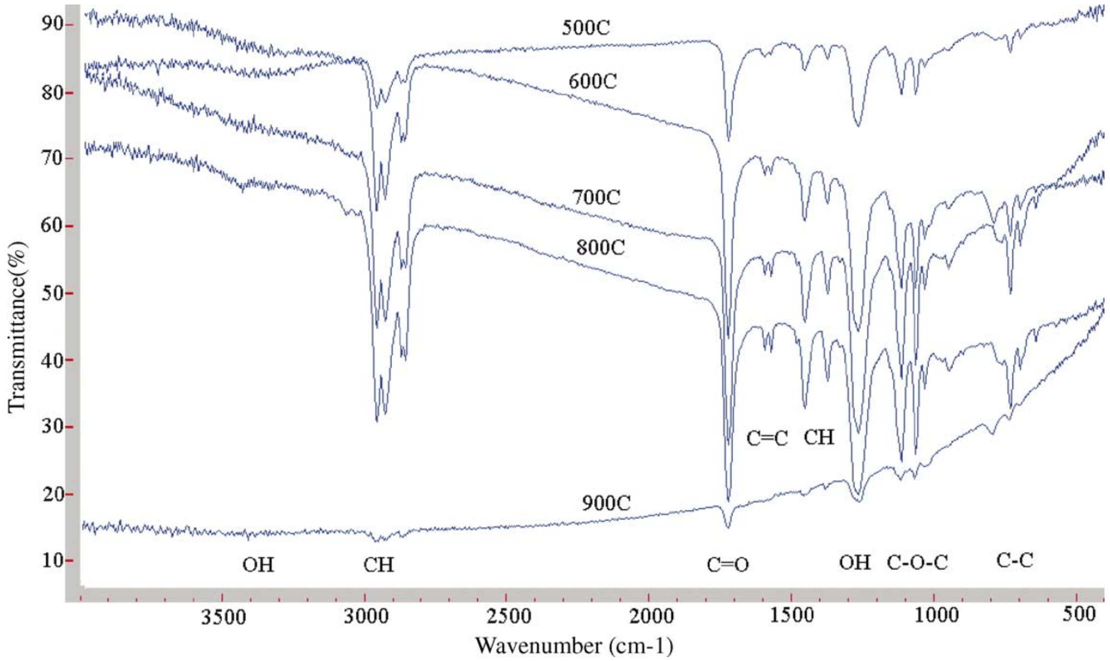

Fig. 2. FTIR spectra of liquid oil from shell pyrolysis at different temperatures.

Table 3
Gas product distribution from shell pyrolysis at different residence times

RT (s)	Components of the gas product (vol.%, N_2- and H_2O-free)						Gas volume (m^3/kg)	LHV (MJ/m^3)
	H_2	CO	CH_4	CO_2	C_2H_4	C_2H_6		
26	14.52	26.83	4.92	52.38	1.33	0.02	0.36	7.6
20	19.20	32.14	5.75	41.56	1.35	0.02	0.37	9.05
14	16.77	32.47	5.79	43.52	1.43	0.02	0.42	8.91
9	33.49	41.33	11.92	10.78	2.46	0.02	0.35	14.67
7.5	37.56	34.69	11.21	13.16	3.36	0.02	0.22	14.60

indicated by the transmittance peaks between 698–900 cm^{-1} and 1420–1610 cm^{-1}. The functional groups observed in the liquid oil from pyrolysis of palm oil shell are compatible with that obtained from hazelnut shell [21].

At 500 °C the IR peak values of transmittance are relatively high, due to possibly the higher water content in the liquid oil compared to other temperatures. The IR transmittances of the above-mentioned functional groups decreased greatly as temperature increased to 600–800 °C, indicating the significant increases of absorbance and thus the great increase of their contents in liquid oil. However, with temperature increased to 900 °C, the IR transmittance peak shrank greatly, due to potentially the thermal cracking of organics inside the liquid oil and thus releasing of more light gas species at high temperature (900 °C). With the great decrease of IR transmittance of functional groups, it can be assumed that a large amount of organics bonds (such as CH, C=O, OH, CC, C–O–C and C–C aromatic ring, etc.) cracked to form light gas products (H_2, CH_4, CO and CO_2, etc.).

3.2. Influence of residence time on shell pyrolysis

Residence time (RT) is another important parameter affecting pyrolysis product distribution [1]. With respect to the existing set-up, the residence times studied are high compared to other reactors, and varied in the range of 7.5 to 26 s. The results of shell pyrolysis at different RTs are listed in Table 3. The total gas yield (in volume) increased first with increasing RTs and reached the maximum of 0.42 m^3/kg at 14 s. Then, it decreased slightly with further increasing of RTs to 26 s. Lengthening the residence time will improve the thermal cracking of heavy hydrocarbon (tar) (Eq. (2)) and some shift reactions (Eqs. (3)–(10)), and therefore more light gas species (H_2, CO, CO_2) are formed. Similar observation was found in a previous publication [4]. But with a further increase of RTs from 14 to 26 s, the total gas volume decreased slightly with unknown reasons. Further study is needed to understand it better.

As for the individual gas species, the H_2 content in Table 3 decreased greatly with RTs increasing, and reached the highest yield of 117.22 ml/g (i.e., 10.40 g/kg, daf) at 9 s. It is different from others' result where the H_2 yield was found to increase with lengthening RTs [3]. Most possibly the considered RTs in this study are too long, causing charcoal reaction with H_2 to form methane. Usually, the residence time of gas vapor is just a few seconds or less in a bench scale reactor such as free wall reactor [4], fixed bed reactor [5], fluidized bed reactor [22], and others [23]. Meanwhile, the CO_2 content increased greatly with RT increasing whilst that of hydrocarbons (CH_4 and C_2H_4) decreased. The content of CO reached the maximum at 9 s. However, the main gas species found in this study (H_2, CO and CO_2) are different from that of Font et al. [23] where the main gas species include C_2H_4 (45 vol.%) and CO (28 vol.%) under the operating condition of achieving the highest gas yield (T @ 890 °C, RT @ 2.3 s). It might be caused by the difference of operating conditions and sample physical–chemical characterizations between these two experiments [24]. From the LHV of the total gas produced, it can be observed that CO_2 played a critical role on the LHV of gas products, which was lowered sharply with increasing CO_2 content. To other gas species (H_2, CO, CH_4, C_mH_n), their contents showed direct proportion to the LHV of gas products.

3.3. Influence of adding catalyst

The results of catalytic pyrolysis of shell at 900 °C are listed in Table 4. All catalysts (C/W=5 wt.%) in Table 4 displayed a more or less positive influence on the total volume of gases produced. In general, Ni appeared to have a stronger catalytic effect than others; with the presence of Ni the total gas yield from shell pyrolysis was increased almost to triple (0.90 m^3/kg) of that without catalyst (0.35 m^3/kg). But dolomite almost exerted no influence on the total gas yield with minor increases (<2 wt.%), possibly because either its load is low or the components of dolomite used are different from that of other literature [25].

As for the individual gas, adding catalysts (except for Na_2CO_3) improved the H_2 content whilst the CO contents were decreased for all the cases, attributed possibly to the shifting reactions (Eqs. (2)–(10)). This changing trend is consistent with that observed from the steam gasification in previous research [26]. The highest H_2 content (38.45 vol.%) was obtained with La/Al_2O_3 as catalyst. For other gas species (CO_2, CH_4, C_2), their contents are varied with adding different catalysts. Adding alkalis (Na_2CO_3, K_2CO_3) decreased greatly the methane content, but improved greatly that of CO_2. It was previously known that alkalis used to weaken the C–C bond [9] to prevent the

Table 4
Gas product distribution from shell pyrolysis with different catalysts

Catalyst	Components of the gas product (vol.%, N_2- and H_2O-free)						Gas volume (m^3/kg)	LHV (MJ/m^3)
	H_2	CO	CH_4	CO_2	C_2H_4	C_2H_6		
No catalyst	33.49	41.33	11.92	10.78	2.46	0.02	0.35	14.67
K_2CO_3	31.42	30.35	7.62	28.74	1.84	0.03	0.53	11.14
$CaMg(CO_3)_2$	36.57	36.61	13.09	10.75	2.89	0.09	0.39	15.15
Na_2CO_3	16.93	27.86	4.78	48.78	1.62	0.02	0.44	8.01
γ-Al_2O_3	34.63	38.81	13.47	11.28	1.72	0.09	0.85	14.61
Fe_2O_3	34.50	38.03	12.31	12.10	2.07	0.99	0.64	14.88
Ni	37.28	38.32	11.47	10.83	2.05	0.04	0.90	14.30
La/Al_2O_3	38.45	36.12	12.00	11.53	1.82	0.07	0.76	14.21

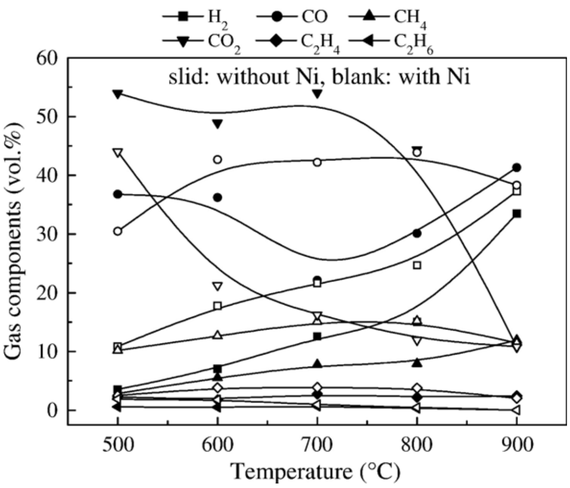

Fig. 3. The comparison of gas products from shell pyrolysis with and without adding Ni.

formation of stable chemical structures by an oxygen transfer mechanism, as such the total gas volume were increased. The gas species distributions are quite similar for cases of adding dolomite, Fe_2O_3, γ-Al_2O_3, La/Al_2O_3 and Ni, although their gas yields are variable, in a descending order of Ni > γ-Al_2O_3 > La/Al_2O_3 > Fe_2O_3 > dolomite. Their gas products contain in general 34–37 vol.% of H_2, 36–38 vol.% of CO, 12 vol.% of CH_4, 11–12 vol.% of CO_2 and the rest are 2–3 vol.% of C_2H_4 and trace C_2H_6. With regards to H_2 production, the highest yield (29.78 g/kg, daf) is found with Ni as catalyst; it almost reached the gasification level (~30 g/kg, daf) [27]. The LHV of gas products is listed in Table 4 as calculated using Eq. (11). The lower heating value of the gas product is about 14–15 MJ/kg except for adding K_2CO_3 and Na_2CO_3 as catalysts.

For further investigation, shell mixed with 5% Ni (C/B = 5%) was pyrolyzed at 500–900 °C in the countercurrent fixed bed reactor. The contents of different gas components that evolved with the presence of Ni are plotted in Fig. 3 (in blank symbol) and compared with that without Ni (in solid symbol). The volume of total gas products and the calculated LHV is shown in Fig. 4 (with Ni — blank symbol and without Ni — solid symbol). With the presence of Ni as a catalyst, the LHV values of gas products are all higher than 11 MJ/m^3 (Fig. 4, indicated by empty symbol) and get the highest of 16 MJ/m^3 at 700–800 °C whilst the highest LHV for the cases without Ni (solid symbol) is slightly above 10 MJ/m^3 only at 900 °C. The total gas volume is also increased sharply with the presence of Ni from 600 °C upwards (Fig. 4). To compare the blank symbols with solid symbols in Fig. 3, with adding of Ni the H_2 content increased largely (~10 vol.%) and CH_4 content also increased ~8 vol.% at different temperatures (500–900 °C), the contents of C_2H_4 and C_2H_6 also showed a slight increase. The CO content was increased (10 vol.%) only at 600–800 °C whilst at 500 °C and 900 °C it decreased slightly (<5 vol.%). In contrast to other gas components, the CO_2 content decreased largely from 38 to 10 vol.% with adding Ni. These changes in gas components contributed to the great increase of LHV of gas products (Fig. 4). Ni exerted a much stronger catalytic influence on gas components at 600–800 °C, indicated also by the big difference of LHV. Although Ni did not show distinct catalytic influence on gas species distribution at 900 °C, it enhanced the total gas yield most greatly at this temperature, most possibly due to the thermal cracking of tar and water shifting reaction occurring at higher temperature (800–900 °C) with the help of catalyst effect of Ni [20,28].

The liquid oils obtained from shell pyrolysis with Ni as catalyst at different temperatures (500–900 °C) were also analyzed using FTIR. Their IR spectra showed similar patterns of IR absorbance of the liquid oil from shell pyrolysis at 900 °C without the presence of catalyst, except that the peak values of the former are much lower. It implied that the liquid oils, from shell pyrolysis with and without Ni as catalyst, contain hydrocarbons with similar functional groups. The decrease of IR absorbance peak values in the case of Ni presence might be caused by the thermal cracking of liquid oil under the help of catalyst (Ni). The catalytic effect due to Ni is significant even at lower temperature (500 °C). It is noteworthy that the performance of Ni as a catalyst in biomass pyrolysis is also influenced by the liquid oil and char deposition. Unfortunately, in this study the yields of tar and coke at different conditions were mostly not recorded, as the focus of this study is H_2-rich gases. But it will be considered in our future research to understand the effect of adding catalyst on the yields of liquid oil and solid coke. The lifetime of catalysts used is another important issue. Nevertheless, as dry-mixed with biomass sample the catalysts were not repeatedly used in this study. The effect of catalyst lifetime will also be investigated in our future work.

Generally, it is difficult for thermal cracking and water gas shift reaction to reach equilibrium during biomass pyrolysis, especially at low temperature (500 °C). However, with the assistance of catalyst, the shift reaction, to a larger degree, could hopefully approach the thermodynamic limit [9]. In this study, a thermodynamic calculation is conducted to predict the gas components from pyrolysis of three palm oil wastes at high operating temperature (900 °C) and long residence time (9 s) as

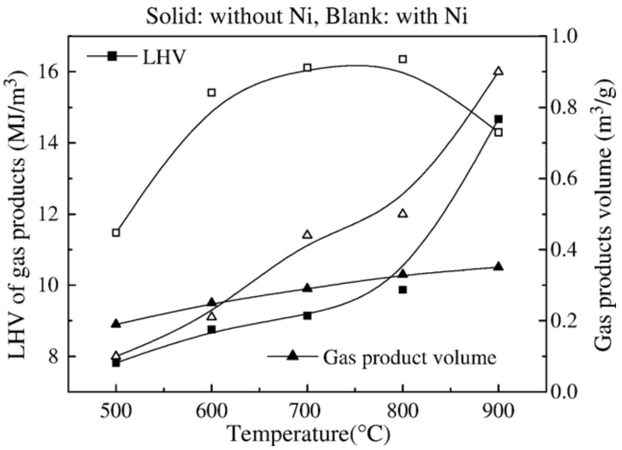

Fig. 4. The comparison of the LHV and total volume of gas products from shell pyrolysis with and without adding Ni.

Table 5
Comparison of the result of thermodynamic calculations and experiments

Sample	Calculated results (vol.%)				Experimental results (vol.%)					
	H_2	CO	CO_2	CH_4	H_2	CO	CO_2	CH_4	C_2H_4	C_2H_6
Shell	60.65	38.22	0.40	0.73	37.28	38.32	11.47	10.83	2.05	0.04
Fiber	60.42	38.45	0.41	0.73	36.72	33.84	11.99	13.36	3.91	0.18
EFB	58.67	40.20	0.45	0.68	36.36	32.65	13.39	14.74	2.78	0.08

well as with the presence of 5 wt.% of Ni — the most effective catalyst. The calculated results are compared with the experimental findings in Table 5. From experimental results, it can be observed that H_2 and CO are the two main components, they covered altogether more than 70 vol.% of gas products. The left part mainly consisted of CO_2 (~10 vol.%), CH_4 (~10 vol.%), C_2H_4 (2–4 vol.%) and a little of C_2H_6. However, from thermodynamic equilibrium calculation the main gas products of palm oil wastes pyrolysis at 900 °C are CO and H_2 with a little of CO_2 and CH_4 [18]. Only ~37 vol.% of H_2 was produced in the experiments. The thermodynamically-favorable production of H_2 at ~60 vol.% has not been achieved, due to possibly certain kinetic constraints. The shift reaction of CH_4 and CO_2 is favored only at low pressure (negative pressure) and high temperature (>1000 °C) [29]. Consequently, at our studied conditions (900 °C and atmospheric pressure), CO_2 and CH_4 could still be the main gas products from palm oil wastes pyrolysis (even with an addition of 5 wt.% Ni).

4. Conclusions

The main products of palm oil pyrolysis are solid charcoal, liquid oil and hydrogen rich gas product. Gas yield increased greatly whilst solid and liquid yields decreased straightly as temperature increases from 500 to 900 °C. The gas products mainly consist of H_2, CO, CO_2 and CH_4 with trace amounts of C_2H_4 and C_2H_6. High temperature is favorable for the enhancement of flammable gas products including H_2, CO and CH_4. Consequently, the LHV of gas products increased greatly with temperature and got 14.57 MJ/m^3 at 900 °C. Residence time also plays a great role on the upgrading of biomass pyrolysis gas product. The contents of H_2 and CO increased as residence time decreased whereas that of CO_2 decreased largely under the condition studied.

Several potential catalysts (Ni, γ-Al_2O_3, Fe_2O_3 and La/Al_2O_3, etc.) have been investigated on improving gas yield and quality. Ni appeared to have the strongest effect on H_2 yield enhancement, and got the maximum H_2 yield of 29.78 g/kg (daf.). With adding Ni (5 wt.%), the total gas yield from shell pyrolysis was improved and gas quality was upgraded greatly, even at lower temperature (600–700 °C). From an energy viewpoint, the heating values of the gases generated in the process are about 14–16 MJ/m^3, which can be used directly for gas turbine, engine, and boiler as gas fuel.

Acknowledgements

The author wishes to express her sincere thanks and appreciation of the financial support from National Nature Science Foundation of China (50446021) and Nature Science Foundation of Hubei province (2003ABA086).

References

[1] A. Demirbas, G. Arin, An overview of biomass pyrolysis, Energy Sources 24 (2002) 471–482.
[2] A.V. Bridgwater, Catalysis in thermal biomass conversion, Applied Catalysis. A, General 116 (1994) 5–47.
[3] X. Dai, C. Wu, H.B. Li, Y. Chen, The fast pyrolysis of biomass in CFB reactor, Energy and Fuels 14 (2000) 552–557.
[4] R. Zanzi, K. Sjostrom, E. Bjornbom, Rapid pyrolysis of agricultural residues at high temperature, Biomass and Bioenergy 23 (2002) 357–366.
[5] F. Ates, A.E. Putun, E. Putun, Fixed bed pyrolysis of *Euphorbia rigida* with different catalysts, Energy Conversion and Management 46 (2005) 421–432.
[6] G. Chen, J. Andries, H. Spliethoff, M. Fang, P.J. van de Enden, Biomass gasification integrated with pyrolysis in a circulating fluidised bed, Solar Energy 76 (2004) 345–349.
[7] S. Li, S. Xu, S. Liu, C. Yang, Q. Lu, Fast pyrolysis of biomass in free-fall reactor for hydrogen-rich gas, Fuel Processing Technology 85 (2004) 1201–1211.
[8] A. Demirbas, Gaseous products from biomass by pyrolysis and gasification: effects of catalyst on hydrogen yield, Energy Conversion and Management 43 (2002) 897–909.
[9] G. Chen, J. Andries, H. Spliethoff, Catalytic pyrolysis of biomass for hydrogen rich fuel gas production, Energy Conversion and Management 44 (2003) 2289–2296.
[10] P.T. Williams, N. Nugranad, Comparison of products from the pyrolysis and catalytic pyrolysis of rice husks, Energy 25 (2000) 493–513.
[11] D. Sutton, B. Kelleher, J.R.H. Ross, Review of literature on catalysts for biomass gasification, Fuel Processing Technology 73 (2001) 155–173.
[12] G. Loffler, V.J. Wargadalam, F. Winter, Catalytic effect of biomass ash on CO. CH4, and HCN oxidation under fluidized bed combustor conditions, Fuel 81 (2002) 711–717.
[13] K. Tomishige, M. Asadullah, K. Kunimori, Syngas production by biomass gasification using Rh/CeO2/SiO2 catalysts and fluidized bed reactor, Catalysis Today 89 (2004) 389–403.
[14] F.A. Agblevor, S. Besler, Inorganic compounds in biomass feedstocks. 1. Effect on the quality of fast pyrolysis oils, Energy and Fuels 10 (1996) 293–298.
[15] H.P. Yang, R. Yan, T. Chin, D.T. Liang, H.P. Chen, C.G. Zheng, TGA–FTIR analysis of palm oil wastes pyrolysis, Energy and Fuels 18 (2004) 1814–1821.
[16] M. Diaz-Somoano, M.R. Martinez-Tarazona, Trace element evaporation during coal gasification based on a thermodynamic equilibrium calculation approach, Fuel 82 (2003) 137–145.
[17] A. Roine, Outokumpu HSC chemistry for windows, Chemical reaction and equilibrium software with extensive thermochemical database, HSC chemistry 4.0, in Outokumpu Research Oy. 1999: Finland.
[18] R. Yan, H.P. Yang, T. Chin, D.T. Liang, H.P. Chen, C.G. Zheng, Influence of temperature on the distribution of gaseous products from pyrolyzing palm oil wastes, Combustion and Flame 142 (2005) 24–32.
[19] A. Demirbas, Yields of hydrogen-rich gaseous products via pyrolysis from selected biomass samples, Fuel 80 (2001) 1885–1891.
[20] P. McKendry, Energy production from biomass (part 3): gasification technologies, Bioresource Technology 83 (2002) 55–63.

[21] A.E. Putun, A. Ozcan, E. Putun, Pyrolysis of hazelnut shells in a fixed-bed tubular reactor: yields and structural analysis of bio-oil, Journal of Analytical and Applied Pyrolysis 52 (1999) 33–49.

[22] S. Rapagna, E. Tempesti, P.U. Foscolo, E. Parodi, Continuous fast pyrolysis of biomass at high temperature in a fluidized bed reactor, Journal of Thermal Analysis 38 (1992) 2621–2629.

[23] R. Font, A. Marcilla, J. Devesa, E. Verdu, Gaseous hydrocarbons from flash pyrolysis of almond shells, Industrial Engineering Chemistry Research 27 (1988) 1143–1149.

[24] D.S. Scott, J. Piskorz, M.A. Bergougnou, R. Graham, R.P. Overend, The role of temperature in the fast pyrolysis of cellulose and wood, Industrial Engineering Chemistry Research 27 (1988) 8–15.

[25] P.A. Simell, J.K. Leppalahti, J.B. Bredenberg, Catalytic purification of tarry fuel gas with carbonate rocks and ferrous materials, Fuel 71 (1992) 211–218.

[26] P. Perez, P.M. Aznar, M.A. Caballero, J. Gill, J.A. Martine, J. Corella, Hot gas cleaning and upgrading with a calcined dolomite located downstream a biomass fluidized bed gasifier operating with steam–oxygen mixture, Energy and Fuels 11 (1997) 1194–1203.

[27] S. Turn, C. Kinoshita, Z. Zhang, D. Ishimura, J. Zhou, An experimental investigation of hydrogen production from biomass gasification, International Journal of Hydrogen Energy 23 (1998) 641–648.

[28] P. McKendry, Energy production from biomass (part 2): conversion technologies, Bioresource Technology 83 (2002) 47–54.

[29] J.M. Encinar, J.F. Gonzalez, J. Gonzalez, Steam gasification of *Cynara cardunculus* L.: influence of variables, Fuel Processing Technology 75 (2002) 27–43.